



Phosphorus fractionation and adsorption characteristics in drinking water reservoir inlet river sediments under human disturbance

Zihao Fu¹ · Zijin Hong¹ · Junling Wei¹ · Yukai Liao¹ · Songlin You¹ · Yifan Wang¹ · Jianjing Lv¹ · Huan Feng² · Marek Kolenčík³ · Xuexiu Chang^{4,5} · Yu Qian^{1,6}

Received: 2 March 2022 / Accepted: 10 June 2022 / Published online: 2 July 2022
© The Author(s), under exclusive licence to Springer-Verlag GmbH Germany, part of Springer Nature 2022

Abstract

Purpose Sediment phosphorus fractionation, adsorption kinetics, and adsorption isotherm characteristics were studied in two rivers, Muyang River and Lengshui River in China, emptying into a drinking water source reservoir, Songhua Reservoir. The relationship between phosphorus fractions and adsorption characteristics was further investigated to explore possible management options for maintaining river water quality.

Methods Sediment samples were collected from six and five sampling sites located along the Muyang and Lengshui Rivers, respectively. Sediment physical–chemical properties and phosphorus fractions were quantified. Adsorption characteristics were modeled with adsorption kinetics and adsorption isotherms.

Results The results from sedimentary sequential chemical extraction (SEDEX) method showed that organic phosphorus (Org-P) had the highest portion of total phosphorus in sediments, followed by detrital phosphorus and authigenic phosphorus (Auth-P), residual phosphorus, iron-bound phosphorus (Fe–P), aluminum-bound phosphorus (Al-P), and exchangeable phosphorus. Notably, the Lengshui River had a higher portion of Fe–P. The kinetics of phosphorus adsorption in sediments was simulated using a pseudo-second-order kinetic model. The results showed that sediment phosphorus adsorption in the upper reaches of the rivers was primarily dominated by single-layer adsorption, whereas that in downstream reaches gradually became irregular and complex deep adsorption. Adsorption isotherms could be well fitted using the modified Langmuir model and the Freundlich model, which indicated that the Lengshui River sediment had higher maximum phosphorus adsorption capacity and strength than Muyang River sediments. The EPC_0 values of sediments in both rivers indicated that sediments acted as the source of phosphorus in surface water. Principal component analysis showed that (i) the portion of Fe/Al-P in sediments positively correlated with equilibrium adsorption capacity, rate, and strength; (ii) Auth-P in sediments could increase the speed and amount of physically adsorbed phosphorus in sediments; and (iii) Org-P positively impacted the maximum adsorption capacity of phosphorus in sediments.

Conclusion Sediment phosphorus fractions and sorption could be affected by human disturbance. At the same time, sediment phosphorus fraction features correlated with several P adsorption characteristics. The findings from this study provide useful guidance for water quality protection of the drinking water source reservoir.

Keywords Sediment · Phosphorus · Adsorption kinetics · Isotherm · Drinking water reservoir

Responsible editor: Shiming Ding

✉ Xuexiu Chang
xchang@uwindsor.ca

✉ Yu Qian
qianyu@ynu.edu.cn

Extended author information available on the last page of the article

1 Introduction

Anthropogenic phosphorus (P) source including human activities such as agricultural production, animal husbandry, and municipal wastewater discharge can contribute P input to aquatic systems (Carpenter 2005). Surface sediment under overlying water can be considered as internal P source

supplying P to the overlying water through benthic-pelagic coupling (Song et al. 2017; Li et al. 2019a; Yang et al. 2020). Once the land-based external loading of P is under control, the release of endogenous P from the sediments will become an important factor restricting water quality recovery (Liu et al. 2016). Phosphorus-enriched sediments are an indispensable component of P internal source and play a critical role in the transport and transformation of P in the aquatic ecosystem. The concentration of P in the overlying water varies with the sediment physical and chemical property change because of benthic-pelagic coupling. Previous studies (Petticrew and Arocena 2001; Zhu et al. 2013; Gao et al. 2016; Yang et al. 2017) showed that P entering rivers was scavenged by the particles through adsorption and accumulated in sediments through natural particle setting due to gravity. The results suggest that sediments can serve as a “phosphorus sink” (Sharpley et al. 2013). However, sediments can also release P into the overlying water, acting as a “phosphorus source” (Søndergaard et al. 2013).

Metal oxides or hydroxides, clay minerals, organic matter, etc. in sediments can determine P fractions in sediments (Reddy et al. 1999; Evans et al. 2004; Su et al. 2014). When P in the overlying water settles into sediments, it will be involved in geochemical reactions with other chemical species, hydrates, clay minerals, and so on and form new P species and minerals stored in sediments (Dittrich et al. 2013). Therefore, knowledge of sediment properties can help to understand the formation and transformation of sediment P fractions.

Investigation of sediment P fractions helps understand P adsorption and release, which has great significance for water environment management (Jin et al. 2013; Dan et al. 2020; Pu et al. 2020). Different P fractions in sediments have different migration and transformation capabilities, bioavailability, and release capabilities (Wang et al. 2006). According to P activity and potential bioavailability, P fractions in sediments can be divided into exchangeable P (Ex-P), iron-bound P (Fe-P), aluminum-bound P (Al-P), calcium-bound P (Ca-P), organic P (Org-P), and residual P (Res-P) (Kaiserli et al. 2002). Among them, Ex-P, Fe-P, Al-P, and Org-P are considered P fractions with higher bioavailability (Rydin 2000; Shinohara et al. 2012; Ni et al. 2020), and their contribution to the surface water P concentration increases significantly. Nevertheless, the extent of sediment P fraction impacting P adsorption behavior under human disturbance has not been well studied yet.

The adsorption of P on sediments is an important process governing P concentration in water bodies. Understanding the characteristics of P adsorption in sediments is crucial for water quality management (Li et al. 2021; Long et al. 2021). The adsorption kinetics and isotherm parameters (e.g., pseudo-second-order kinetic model and Langmuir model) are frequently used to characterize sediment P adsorption.

Many factors can affect the characteristics of P adsorption in sediments, including environmental factors such as temperature, pH, DO, and biological factors (Barbosa et al. 2020; Cai et al. 2020; Gautreau et al. 2020). However, there have been few studies on the effect of background P fractions on P adsorption characteristics in sediments, and the contribution of specific P fractions to the sediment adsorption process is currently under debate. On the one hand, studies showed that sediment P fraction formation varied with sediment P adsorption processes, which is mainly determined by sediment composition and surface characteristics. For example, sediments rich in calcium carbonate tend to form Ca-P after P adsorption (Wang and Lin 2010), while sediments that have rich hydroxide groups on surface tend to form Ex-P and Fe-P after P adsorption (Cao et al. 2017). On the other hand, human disturbance may change the composition of sediment P fractions, further alter sediment P adsorption behavior, and then increase the risk of sediment P release. For example, Fe/Al-P has high adsorption rate and low desorption rate during chemical adsorption process in sediment. Hence, it can affect the maximum P adsorption capacity of sediment (Wang et al. 2012, 2018). Therefore, it is necessary to investigate how sediment P fraction can influence sediment P adsorption. Studying the relationship between sediment P fractions and P adsorption characteristics will be helpful to evaluate the potential of P release from sediment with various P fraction features, and further provide valuable support for water quality protection and sediment P restoration projects.

Songhua Reservoir, located upstream of Dian Lake, is one of the important drinking water sources in Kunming within the Dian Lake Basin. Water quality and safety of the reservoir are closely related to drinking water safety of Kunming City and protection of the Dian Lake ecosystem. The main replenishment tributaries of the reservoir are the Muiyang River and Lengshui River. However, since there are several residential and farming areas within the watershed of these two rivers, the water quality of the two rivers is threatened by both point sources (e.g., domestic sewage) and non-point source (e.g., agricultural planting, livestock, and poultry grazing) pollution. Therefore, the water quality of these rivers has been decreasing dramatically in recent years, posing a new challenge to Songhua Reservoir water quality management. Although phosphorus is an essential limiting nutrient for algal blooms, water quality monitoring of river channels shows that some river channels have high concentrations of the total P (TP) (Yuan 2019). Therefore, it is necessary to pay attention to the pollution of P in the two rivers.

Recent studies in the Muiyang River and Lengshui River are primarily focused on water quality safety (Hong et al. 2012; Qiu et al. 2012) with few causes focusing on river sediments. In addition, most of the studies on the Dian Lake

Basin are focused in the Dian Lake, with few studies focusing on the upper reaches of the Dian Lake (Le et al. 2010; Yan et al. 2019). To aid in the organization of water quality maintenance practices and the establishment of water quality deterioration early warning systems, a series of sediment physical–chemical properties, including nutrient chemical concentration P fraction and P adsorption/desorption characteristics, should be investigated. In particular, when sediment particles are resuspended, P adsorbed by sediments (especially the active P fractions) will be released back into water body and cause an increase of P concentration in the water body (Selig 2003; Li et al. 2019c). Therefore, exploring the relationship between P adsorption characteristics and sediment P fractionation can not only unveil the possible mechanism of how sediment properties impact P adsorption, but also provide valuable information for river sediment remediation and management in the drinking water reservoir protection areas.

The objectives of this study are to (i) investigate the sediment properties, P composition, and P adsorption characteristics of the inflow channel of Songhua Reservoir; (ii) explore the relationship between sediment properties and P components, as well as P components and P adsorption characteristics; and (iii) propose targeted water quality protection approaches with respect to the current human interference situation. This goal is to fill the gap in understanding sediment function in the upper reaches of Dian Lake, provide effective approaches for water quality control and safety protection, and improve the water pollution status of Songhua Reservoir.

2 Materials and methods

2.1 Study site and sample collection

Songhua Reservoir covers an area of 629.8 km² and is located between 102°54′–102°59′ E and 25°10′–25°28′ N. The Muiyang River is 48.15 km long in length and has a drainage area of approximately 346.82 km². The average precipitation in this area is approximately 241 mm. The annual average flow rate is approximately 210×10^6 m³ year⁻¹ with a maximum flow of 122 m³ s⁻¹, and a minimum flow of 0.002 m³. There are 32,615 residents living in approximately 93 villages within the Muiyang River drainage area. The Lengshui River features a total length of 14.5 km, a total runoff area of approximately 111.4 km², an average precipitation of approximately 667 mm, and a flow rate ranging from 0.5 to 67.2 m³ s⁻¹ with an annual average load of approximately 74×10^6 m³ year⁻¹. There are 41,541 residents distributed in approximately 39 villages within the Lengshui River runoff area. According to the land use and land cover types (i.e., upper reach of the

river without anthropogenic interference, residential areas, agricultural areas, and the ecological recovery area in the inlet of the water reservoir), six and five sampling sites were established along the Muiyang and Lengshui Rivers, respectively. Among the six sample sites in the Muiyang River, site A1 was located in the upper river area and was free of human disturbance, sites A2, A3, and A4 were located in areas with intense inhabitant or agricultural activity, site A5 was located at an intersection where small tributaries joined the main river, and site A6 was established above the reservoir entrance (Fig. 1). Among the five sampling sites in the Lengshui River, site B1 was near a temple with a well-preserved environment, sites B2 and B3 were near residential areas, where villages and farmlands gathered, site B4 was within the ecological recovery area intended to reduce water contaminants, and site B5 was directly above the reservoir entrance (Fig. 1).

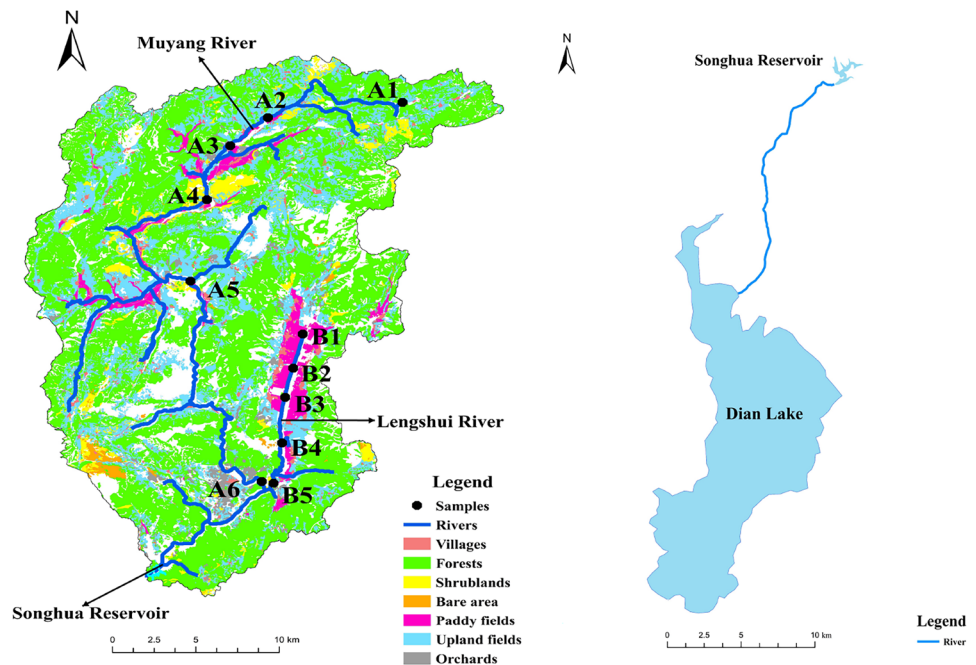
Surface sediment samples were collected in November 2020. Because the water depth of the river was shallow (average depth 20 cm), the surface sediments were excavated manually by using shovel in the river. The surface sediments (0–5 cm) were excavated as sediment samples. A detail description of the sample location is given in the supplementary material (SI). The collected sediment samples were sealed in a 1-L polyethylene plastic bottle that was cleaned and rinsed on-site, placed in an ice container, stored at 4 °C for preservation, and then transported to the laboratory in the Yunnan University. Before chemical analysis, the sediment samples were freeze-dried in a freeze dryer for 24–48 h, ground through a 100-mesh sieve, and then stored at 4 °C for analysis.

2.2 Sediment property measurement

Sediment total nitrogen (TN), NO₃⁻, NO₂⁻, NH₄⁺, and TP concentrations were determined using sulfuric acid digestion-sodium salicylate method (Lao 1988), hydrazine sulfate reduction method (EPA-METHOD #: 353.2) (USEPA 1993), diazo coupling method (HJ634-2012) (EPD 2012), sodium salicylate method (HJ634-2012) (EPD 2012), and sulfuric acid digestion-molybdenum antimony method (Lao 1988) analysis, respectively. Sediment pH was measured after shaking the soil solution with a ratio of sediment:water = 1:2.5 for 30 min (Dai et al. 2020). Sediment organic matter was determined using the gravimetric method (LY/T 1237-1999) (NFB 1999). The concentrations of total iron (TFe₂O₃), CaO, and Al₂O₃ in sediments were determined using an X-ray fluorescence spectrometer (GB/T 14506.28-2010) (GAQ and SA 2010).

The improved sedimentary sequential chemical extraction (SEDEX) method was used to determine P fractions in the sediment samples (Ruttenberg 1992; Vink et al. 1997; Li

Fig. 1 The sampling sites



et al. 1998). A description of detailed extraction procedure is given in the supplementary material (SI).

2.3 Sediment phosphorus adsorption characterization

2.3.1 Adsorption kinetics

Three 50-mL centrifuge tubes were prepared for each sample point followed by adding an aliquot of 0.20-g sediment sample and a 20-mL phosphate standard solution (KH_2PO_4) with an initial concentration of 1 mg L^{-1} . The pH value of the solution was adjusted using dilute hydrochloric acid or dilute sodium hydroxide to approximately 7.00. To avoid interference from different ions and microorganism growth during the sediment adsorption experiment, 0.01 M KCl and 0.1% chloroform were added to the phosphate solution. The centrifuge tubes were oscillated at a constant temperature of $25 \text{ }^\circ\text{C}$ and 200 rpm for 30 min, 1 h, 2 h, 4 h, 6 h, 9 h, 12 h, 24 h, 48 h, and 72 h, respectively. Then, the supernatant and sediment in the tubes were separated by centrifugation in a centrifuge at $5,000 \text{ r min}^{-1}$ for 5 min at each time interval. Then, 2 mL of the supernatant was collected from each tube and filtered through a $0.45\text{-}\mu\text{m}$ filter membrane before phosphate concentration measurement on an automatic discontinuous chemical analyzer (Cleverchem380, DeChem-Tech GmbH, German) (Xie et al. 2019). Three centrifuge tubes without sediment were processed simultaneously as a blank control.

To investigate the characteristics of adsorption kinetics, we fitted our data to three adsorption models and compared

models. The kinetic processes of phosphate adsorption on sediments can be described using the pseudo-first-order reaction kinetics model, pseudo-second-order reaction kinetic model, and the Elovich model (Padmesh et al. 2005; Zhu and Yang 2018) in order to examine the controlling mechanisms of the adsorption process (Köse and Kivanç 2011). According to the pseudo-first-order kinetic model, the adsorption process is dominated by physical adsorption (Lagrergen 1898; Pereira et al. 2018). According to the pseudo-second-order adsorption kinetics linear equation, the adsorption process is dominated by chemical adsorption (Ho 2006; Liu et al. 2019b). According to the Elovich model, the adsorption process is a single-layer or multilayer adsorption with irregular surfaces (Liu et al. 2019a; Habte et al. 2020). Commonly, the closer to 1 the fitting value r^2 is, the better the fitting effect is. Thus, the model can better reflect the characteristics of adsorption kinetics.

The adsorption capacity (Q) has been introduced to describe the sediment adsorption effect of P, which predicts the adsorber P quality per unit mass of sediments. The equation for calculating Q is as follows:

$$Q = \frac{(C_0 - C_t) \times V}{\omega} \quad (1)$$

where Q is adsorption capacity in mg kg^{-1} , C_0 is phosphate mass concentration in the initial solution in mg L^{-1} , C_t is mass concentration of phosphate in solution at time t in mg L^{-1} , V is volume of phosphate solution added in mL, and ω is added sediment mass in g.

The Lagergren pseudo-first-order adsorption kinetics linear equation is given as below (Lagergren 1898):

$$\lg(q_e - q_t) = \lg q_e - \frac{k_1}{2.303} t \quad (2)$$

$$\ln(q_e - q_t) = \ln q_e - k_1 t \quad (3)$$

where q_e is P adsorption in sediments at equilibrium in mg kg^{-1} (referring to the amount of P adsorption), q_t is P adsorption in the sediment at time t in mg kg^{-1} , and k_1 is the first-order adsorption rate constant in L min^{-1} (referring to the speed of the adsorption rate during the physical adsorption process).

The Lagergren pseudo-second-order adsorption kinetics linear equation (Ho and McKay 1999) is.

$$\frac{t}{q_t} = \frac{1}{k_2 q_e^2} + \frac{1}{q_e} t \quad (4)$$

where q_e is P adsorption in sediments at equilibrium in mg kg^{-1} (referring to the amount of P adsorption), q_t is P adsorption in the sediment at time t in mg kg^{-1} , and k_2 is the second-order adsorption rate constant in g (mg h)^{-1} (referring to the speed of the adsorption rate in the chemical adsorption process).

The Elovich model (Li et al. 2019b) is given as.

$$q_t = \frac{1}{a} \ln(k_3 a) + \frac{1}{a} \ln t \quad (5)$$

where q_t is P adsorption in the sediment at time t in mg kg^{-1} and k_3 is apparent adsorption rate constant (referring to the speed of P adsorption in the irregular deep adsorption process).

2.3.2 Adsorption isotherm

A total of 18 polyethylene centrifuge tubes (50-mL volume) were prepared for each sample point. An aliquot of 0.20 g of the sediment sample was added to each tube followed by injecting 25 mL of phosphate standard solution with different initial concentrations, i.e., 0, 2, 4, 6, 8, and 10 mg L^{-1} , to the tubes in triplicate. 0.01 M KCl and 0.1% chloroform were added to adjust pH of the solution following the same protocol used for the adsorption kinetics experiment. After a constant temperature oscillation adsorption equilibrium time at 25 °C and 200 rpm for 48 h, the sample was centrifuged at 5,000 r min^{-1} for 5 min, and the supernatant was passed through a 0.45- μm filter membrane before measuring the final phosphate concentration in the solution using an automatic discontinuous chemical analyzer (Cleverchem380, DeChem-Tech.GmbH, German) (Tang et al. 2014).

A modified Langmuir model was proposed by Zhou et al. (2005) who considered the influence of the adsorbate contained in the adsorbent during the adsorption process while describing the sediment P adsorption process. The modified Langmuir model assumes that the adsorbent surface can provide limited adsorption sites with uniform coverage, and the adsorption activation energy of each adsorption site is homogeneous. Hence, the adsorbate can maintain its specific molecular area after being adsorbed on the adsorbent (Hu et al. 2018), i.e., the adsorption sites will not interfere with each other, and each site will not be interfered with other adsorbed molecules after it is combined with the adsorbate. The adsorption process occurs only at the surface monomolecular level so that the maximum adsorption capacity at saturation can be predicted (Habte et al. 2020). The modified Langmuir model is given as follows (Zhou et al. 2005):

$$S = \frac{S_{\max} \times C}{k_4 + C} \left(\frac{S_{\max} \times C^0}{k_5 + C^0} + S^0 \right) \quad (6)$$

where S is phosphate content adsorbed by the sediment at equilibrium in mg kg^{-1} , S_{\max} is the maximum phosphate content that can be adsorbed on the sediment in mg kg^{-1} (referring to the maximum P adsorption capacity), C is the residual phosphate concentration in the overlying water at equilibrium in mg L^{-1} , k_4 is empirical constant in mg L^{-1} (rate constant of adsorption in regular monolayer adsorption process), C^0 is phosphate concentration in the overlying water of the experimental system with an initial P concentration of 0 mg L^{-1} at the moment of equilibrium in mg L^{-1} , S^0 is the P content adsorbed by the sediment at the equilibrium in the experimental system with an initial P concentration of 0 mg kg^{-1} . Furthermore, two parameters are defined as below:

$$\text{NAP} = \frac{S_{\max} \times C^0}{k_4 + C^0} + S^0 \quad (7)$$

where NAP is Ex-P adsorbed by sediment background in mg kg^{-1} , and the other parameter are the same as defined before.

$$\text{EPC}_0 = \frac{k_5 \times S_{\max} \times C^0 / (k_5 + C^0) + k_5 \times S^0}{k_5 \times S_{\max} / (k_5 + C^0) - S^0} \quad (8)$$

where EPC_0 is zero equilibrium P concentration, which means that when the sediment is in contact with a specific concentration of phosphate in water, the sediment neither adsorbs nor desorbs P (Taylor and Kunishi 1971; Froelich 1988; Simpson et al. 2021). In general, when $\text{EPC}_0 >$ overlying water-soluble reactive P (SRP), the sediment is a phosphorus source. However, when $\text{EPC}_0 <$ overlying water SRP, the sediment is a phosphorus sink (Pan et al. 2013).

Besides the modified Langmuir model, the Freundlich model was used to characterize the phosphate adsorption process by sediments, mainly because the model can fit various natural solid-solute systems (Li and Werth 2002). Therefore, it is in common use for describing the phosphate adsorption process in sediments (Leote et al. 2013). The Freundlich model assumes that the adsorbent can provide unlimited heterogeneous adsorption sites, and the binding affinity of an adsorption site on the adsorbent surface will change with the interaction between the adsorbent and adsorbate, and the adsorption process is not limited to only the surface (Wang et al. 2019a; Li et al. 2020). The Freundlich model is expressed as follows (Li et al. 2020):

$$\lg q_e = \lg K_F + \frac{1}{n} \lg C_e \quad (9)$$

where q_e is P adsorption in sediments at equilibrium in mg kg^{-1} , C_e is P solution concentration at equilibrium in mg L^{-1} , K_F is the distribution constant (referring to the strength of the adsorption capacity in the heterogeneous multilayer adsorption process), $\frac{1}{n}$ is an adsorption constant (referring to the adsorption process adsorption binding strength in the heterogeneous multilayer adsorption process).

K_F can reflect the adsorption capacity of the adsorbent to the adsorbate; $\frac{1}{n}$ reflects the strength of the adsorption process. The smaller the $\frac{1}{n}$, the easier the adsorption reaction is. When $0.1 < \frac{1}{n} < 0.5$, the reaction is easy to proceed; when $\frac{1}{n} > 2$, the adsorption reaction is not easy to occur.

2.4 Statistical analysis

Principal component analysis (PCA) and linear correlation analysis were performed using JMP 13 software (SAS Institute Inc.). The significance of linear regression correlation between groups was judged using $p < 0.05$ as the criteria of significance level. Adsorption kinetics and isotherm fitting were performed using SigmaPlot 14.0. Figures were made with Origin 2021.

3 Results and discussion

3.1 Physical–chemical properties of river sediments

The physical and chemical properties of the collected sediments from 11 sampling sites in the two rivers are presented in Table 1. In general, the concentrations of nitrogen, phosphorus, and organic matter in the sediments of the Lengshui River are higher than those in the Muyang River, possibly due to more intensive human activities intensity in the Lengshui River watershed (Fig. 1). As shown in Table 1 and Fig. 1, when the two rivers pass through villages and towns, TP and TN concentration in the sediments increase significantly, which can be attributed to discharge of domestic sewage and agricultural non-point source pollution. Previous studies (Duan et al. 2019; Du 2020) have shown that N and P loads from agricultural non-point source pollution in the basin are higher than that from domestic sewage. The contribution from agricultural non-point sources to TN pollution accounts for 73.66%, of which livestock and poultry manure pollution accounts for 40.23%. In terms of TP pollution, agricultural non-point source contributes 88.99%, of which livestock and poultry manure pollution accounts for 53.76%. Domestic sewage contributes 4.86% of TN pollution and 3.26% of TP pollution (Bao et al. 2015). Sediment TP and TN concentrations in the Lengshui River are higher than those in the Muyang River because the density of farmland and livestock and poultry breeding around the Lengshui River is higher than that around the Muyang River (Fig. 1). Notably, TP concentrations at sites B1–B4 in the Lengshui River shows an increase from upstream to downstream, but a decrease in the reduction area (site B5) before entering the reservoir. As for the TN, it decreases from upstream to downstream in the paddy field area (sites B1–B3) but increases when flowing through forests (sites B4 and B5). It is speculated that P in the water body passing through the

Table 1 The detection results of basic physical and chemical indications of the Muyang River (A1–A6) and the Lengshui River (B1–B5) sediments

Site	TP (mg/kg)	TN (mg/kg)	OM g/kg	CaO %	TFe ₂ O ₃ %	Al ₂ O ₃ %	pH
A1	518 ± 5.94	450 ± 211	9.37 ± 1.81	8.95 ± 1.97	3.15 ± 0.12	7.21 ± 0.30	7.57 ± 0.14
A2	808 ± 64.6	1025 ± 282	16.0 ± 7.50	3.36 ± 0.56	3.98 ± 0.17	11.6 ± 0.70	7.49 ± 0.07
A3	565 ± 27.0	1062 ± 308	10.8 ± 0.97	3.00 ± 2.17	3.95 ± 0.86	10.9 ± 2.23	7.56 ± 0.03
A4	726 ± 29.5	1915 ± 335	30.5 ± 4.25	5.52 ± 1.29	3.44 ± 0.06	10.1 ± 0.69	7.55 ± 0.08
A5	894 ± 39.1	2332 ± 788	22.4 ± 3.22	4.27 ± 0.45	5.80 ± 0.61	12.5 ± 0.40	7.58 ± 0.005
A6	927 ± 37.4	3082 ± 447	22.7 ± 1.22	3.28 ± 0.79	5.99 ± 0.38	14.5 ± 0.83	7.72 ± 0.07
B1	807 ± 47.7	2457 ± 305	48.5 ± 11.0	18.1 ± 0.85	7.00 ± 0.61	11.5 ± 1.02	7.35 ± 0.04
B2	1174 ± 8.07	1085 ± 113	25.5 ± 1.18	4.44 ± 0.20	13.3 ± 0.26	19.6 ± 0.21	7.76 ± 0.06
B3	1423 ± 51.9	1147 ± 291	20.8 ± 1.12	2.22 ± 0.08	9.29 ± 0.14	14.3 ± 7.51	7.48 ± 0.06
B4	1634 ± 86.5	3850 ± 116	53.5 ± 10.3	6.17 ± 0.60	9.68 ± 0.59	13.6 ± 0.56	7.23 ± 0.04
B5	1101 ± 20.8	2764 ± 201	38.3 ± 1.70	3.86 ± 0.19	8.85 ± 0.44	11.6 ± 0.52	7.42 ± 0.02

residential area are largely adsorbed by the sediment, while natural reduction area may provide extra N to the waterbody.

Sediment CaO, TFe₂O₃, and Al₂O₃ concentration in the Lengshui River are higher than those in the Muyang River, indicating that the geological settings of these two rivers are different. When the two rivers pass through the farmland area, the mineral contents in the sediments increase possibly because of the soil loss caused by watering and rainfall, as the farmland is planted directly on the banks of two rivers. According to previous studies (Zhou et al. 2015; Ren and Fu 2017), soil erosion in the basin is severe because the basin is mainly planted. To improve the survival and quality of life, there are deforestation and wasteland in the region (Zhou et al. 2015; Ren and Fu 2017; Wang et al. 2019b). Because the farmland density around the Lengshui River is higher than that around the Muyang River, sediment CaO, TFe₂O₃, and Al₂O₃ concentrations in Lengshui River are higher than those in the Muyang River.

3.2 Sediment phosphorus fraction

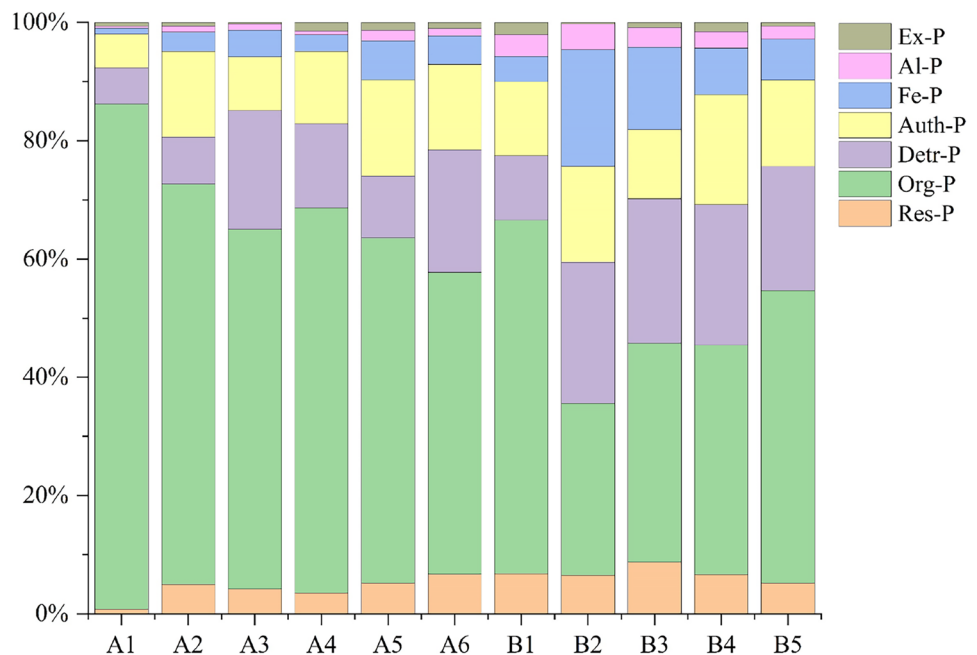
The percentage of each P fraction in sediments from the 11 sites is shown in Fig. 2. Among all P fractions, Org-P and Detr-P have the highest proportion, followed by Auth-P, Fe-P, Res-P, and Al-P, whereas Ex-P has the lowest proportion. Note that the proportion of each P fraction in the sediments varies significantly with the location. According to previous study on pollution load from the river input of Songhua Reservoir, 92.14% of TP pollution load were from non-point source pollution, which was composed of agricultural planting fertilizer loss (61.13%), livestock farming (22.45%),

and domestic sewage (16.42%) (Du 2020). Previous studies indicated that the domestic sewage tends to increase sediment Fe/Al P (Ni et al. 2020; Xiong et al. 2021), fertilizer might increase phytate P (Turner et al. 2003; Copetti et al. 2019), and animal excrement contributed the most to Res-P in sediment (Ni et al. 2016). In this study, further analysis is conducted to show how P fraction in sediment varies with the potential P discharge sources from each study site.

Ex-P is a P fraction that appears to be loosely bound to sediments and highly susceptible to being released when environmental factors (i.e., pH, Eh, temperature, and human disturbance) change (Logan 1982; Zhang et al. 2012). Figure 2 shows that when the two rivers pass through the residential areas (A2, A3, and B2), the proportion of Ex-P in sediments is very small, which is likely to be released by the interference of human activities. This is consistent with the previous findings in relationship between P composition and anthropogenic activities in Jiaozhou Bay sediments (Kang et al. 2017).

Al-P and Fe-P are P fractions combined with aluminum and iron metal oxides or hydroxides in sediments, which can be easily decomposed in alkaline environments because they are easily released by OH⁻ exchange (Jin et al. 2006; Smolders et al. 2006). Furthermore, Fig. 2 shows that Fe/Al-P content in sediments is relatively high in the residential areas (sites A2, A3, and B2). Numerous studies (Ruban et al. 2001; Ni et al. 2020; Xiong et al. 2021) have shown that Fe/Al-P content in sediments is generated from human activities, especially from domestic sewage and industrial wastewater discharge. Comparing the Fe/Al-P contents in the sediments of the two rivers, the Lengshui River has higher TFe₂O₃ and Al₂O₃ concentrations than the Muyang

Fig. 2 Percentage of each phosphorus fractions in sediments of the Muyang River (A1–A6) and Lengshui River (B1–B5) using SEDEX method



River, which is consistent with the relatively higher intensity of anthropogenic activities and pollution degree along the Lengshui River.

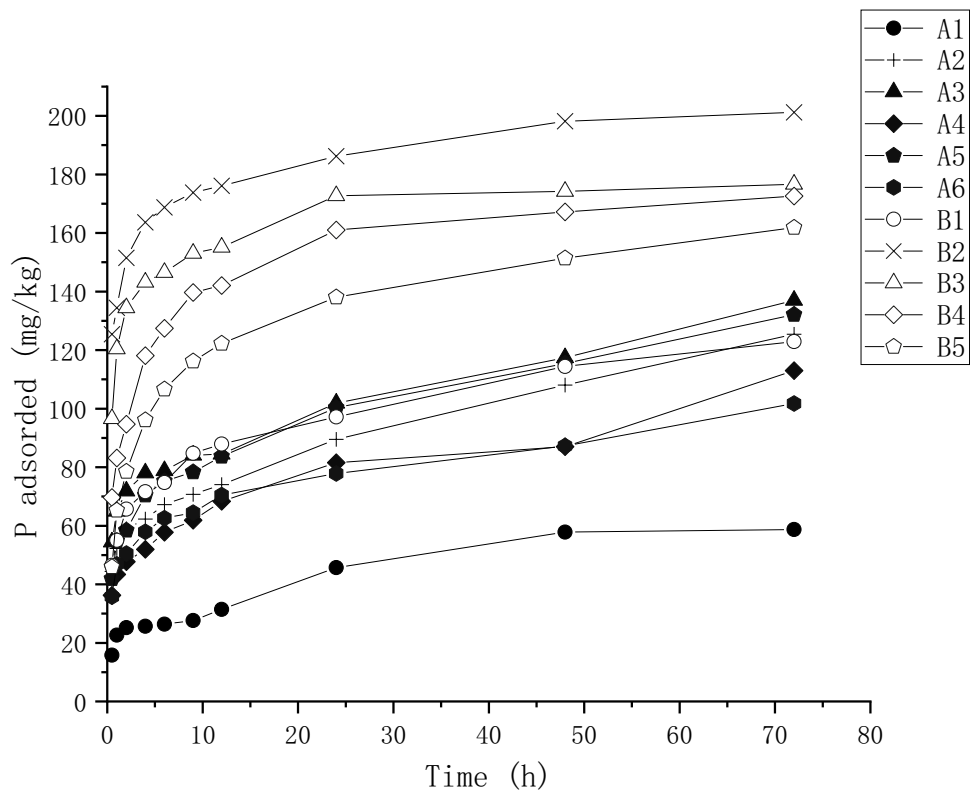
Auth-P and Detr-P are mainly referred to P fractions adsorbed or co-precipitated with calcium compounds in sediments (Loh et al. 2020). Both Auth-P and Detr-P have low sensitivity to environmental change (Kim et al. 2003), and they are extremely stable under alkaline conditions (Kaiserli et al. 2002). Figure 2 shows that the proportion of Auth-P remain relatively stable across different sites, indicating that human activities have little impact on it. The content of Detr-P, however, was higher in the downstream sediments compared to the upstream sediments, possibly due to the occurrence of terrigenous input from soil erosion along the river basin (Vink et al. 1997). Therefore, the variation in Detr-P proportion may indicate the level of soil erosion along the river basin (Meng et al. 2015; Acharya et al. 2016).

Org-P is referred to the P fraction in aquatic biological cells, debris, humus, etc. Generally, there is a positive correlation between Org-P and organic matter (Abeyasinghe et al. 1996; Kastelan-Macan and Petrovic 1996). In addition, because Org-P can be easily released from sediments when the hydrodynamic condition changes or bioturbation occurs (Feng et al. 2018), human disturbance and water velocity may also affect Org-P content in sediment. In this study, no significant correlation ($p = 0.115 > 0.05$) was observed between sediment Org-P and organic matter,

indicating human disturbance and water flow velocity might be the main factors that affect Org-P content in sediment. The highest Org-P content is found in sediments from the pristine upstream area (sites A1 and B1), possibly due to less human disturbance and slower water velocity. Similarly, Org-P content increases at downstream sites (sites B4 and B5), which are the subduction zone with slow water flow velocity and little human disturbance (Figs. 1 and 3). Org-P content in the sediments is relatively low when passing through the residential areas (sites A3 and B2), indicating that human interference may have promoted the release of Org-P in the sediments.

Res-P is mainly composed of non-decomposable inorganic P and insoluble Org-P. It is very stable and difficult to be released into the environment under normal conditions (Meis et al. 2012). Most of the P in agricultural fertilizer and animal excrement exists as monoester P (phytate P) (Turner et al. 2003; Copetti et al. 2019), which usually constitutes the largest part of Res-P in sediment (Ni et al. 2016). Therefore, agricultural P fertilizer application and animal husbandry P emissions can increase the content of Res-P component in sediments (Ni et al. 2020). However, although there are large-scale agricultural planting and several livestock and poultry breeding in the Songhua Reservoir watershed, their impact on Res-P content in sediments is relatively small, which may be due to the control measures of agricultural non-point source pollution in the watershed.

Fig. 3 Sediment phosphorus adsorption kinetics of the Muyang River (A1–A6) and the Lengshui River (B1–B5)



3.3 Sediment phosphorus adsorption kinetics

Figure 3 shows the stages of the P adsorption by the sediments. The P adsorption process is very rapid within 0–10 h, during which sediments can absorb a large amount of P. The adsorption process then become slow within 10–50 h, during which the rate of P adsorption by sediments slows down. The P adsorption equilibrium is reached after 50 h. The maximum equilibrium concentration of P adsorption can reach approximately 200 mg kg^{-1} , whereas the lowest equilibrium concentration of P adsorption is about 50 mg kg^{-1} . In general, the equilibrium concentration of P adsorption by sediments in the Lengshui River is higher than that in the Muyang River (Fig. 3).

The adsorption kinetic characteristics of sediments in Songhua Reservoir can be described in terms of the numerical value of the adsorption kinetic model. In this study, three kinetic models (the pseudo-first-order kinetic model, the pseudo-second-order kinetic model, and the Elovich model) are used to fit the adsorption characteristics of P. If the fitting value r^2 is closer to 1, it suggests that the adsorption kinetics model is close to the actual value, indicating that the model is more suitable for describing the adsorption of sediments (Table 2).

Table 2 illustrates that among the three kinetic models, the pseudo-second-order kinetic model fits the data the best, indicating that the P adsorption process of sediments in the study area is more in line with the pseudo-second-order kinetics. Since the pseudo-second-order kinetic model is developed on the basis of electron transfer forming chemical bonds (Ho and McKay 1999), the P adsorption process in sediments of this study is dominated by surface chemical adsorption, which is dominated by electron transfer to form chemical bonds. Note that the r^2 value of the Elovich model

gradually increases from upstream to downstream, indicating that the adsorption process gradually changes from simple surface monolayer chemical adsorption to complex surface irregularity and deep adsorption (Habte et al. 2020).

In the pseudo-second-order kinetic model, q_{e2} represents the amount of P adsorbed per unit mass of sediment when P adsorption reaches equilibrium, whereas k_2 represents the second-order adsorption reaction rate constant (Ho and McKay 1999). In this study, the average value of q_{e2} in the Muyang River is 111 mg kg^{-1} , whereas the average value of q_{e2} in the Lengshui River is 169 mg kg^{-1} , indicating that sediments in the Lengshui River can adsorb more phosphorus. The average value of k_2 in Muyang River is 0.0021 while the average value of k_2 in the Lengshui River is 0.0036, indicating that the rate of P adsorption by the sediments in the Lengshui River is higher than that in Muyang River, and adsorption equilibrium can be reached in a shorter time. Based on the results of *t*-test, the q_{e2} and k_2 for the Lengshui River are significantly greater than those of Muyang River ($p < 0.05$). Therefore, the P adsorption capacity of sediments in the Lengshui River is stronger than that in the Muyang River.

3.4 Sediment phosphorus adsorption isotherm

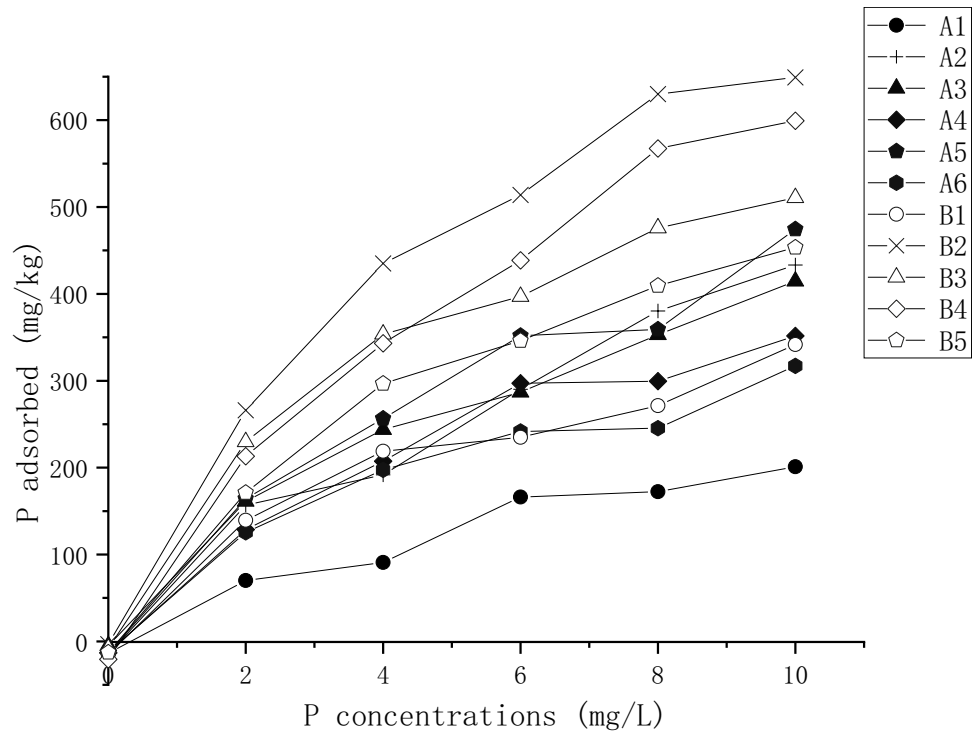
According to the P adsorption isotherm of river sediments (Fig. 4), the Lengshui River sediments have a larger P adsorption capacity than the Muyang River. When the P concentration in the solution is 0 mg L^{-1} , the sediment releases its phosphate, and the adsorption capacity is negative at this time. The P adsorption capacity significantly increased when the phosphate concentration is $2\text{--}8 \text{ mg L}^{-1}$. When the phosphate concentration of the solution is 10 mg L^{-1} , the adsorption reaches saturation.

Table 2 Parameters of P adsorption kinetics on sediments of the Muyang River (A1–A6) and the Lengshui River (B1–B5)

Site	Pseudo-first-order kinetic model			Pseudo-second-order kinetic model			Elovich model	
	q_{e1}	k_1	r^2	q_{e2}	k_2	r^2	k_3	r^2
A1	40.3	0.0459	0.928	62.9	0.0026	0.975	65.1	0.849
A2	57.8	0.0478	0.974	126	0.0017	0.980	349	0.898
A3	54.8	0.0521	0.946	136	0.0019	0.983	845	0.904
A4	50.8	0.0903	0.990	110	0.0019	0.970	231	0.904
A5	64.5	0.0615	0.969	133	0.0018	0.987	303	0.955
A6	42.2	0.0672	0.948	101	0.0029	0.988	427	0.965
B1	57.3	0.0554	0.923	125	0.0025	0.993	530	0.978
B2	55.7	0.0715	0.886	203	0.0046	0.999	122828	0.989
B3	69.7	0.150	0.951	179	0.0057	0.999	34085	0.954
B4	88.2	0.113	0.983	175	0.0031	0.999	1080	0.984
B5	85.9	0.0834	0.953	164	0.0021	0.998	367	0.999

q_{e1} the mass of adsorbed P per mass unit at equilibrium of pseudo-first-order kinetic model (mg/kg), k_1 the empirical constant of pseudo-first-order kinetic model (1/h), q_{e2} the mass of adsorbed P per mass unit at equilibrium of pseudo-second-order kinetic model (mg/kg), k_2 the empirical constant of pseudo-second-order kinetic model (g/mg*h)

Fig. 4 Sediment adsorption isotherm of the Muyang River (A1–A6) and the Lengshui River (B1–B5)



The adsorption isotherm characteristics of sediments in Songhua Reservoir can be described on the basis of the value of the adsorption isotherm model. To explore the characteristics of P adsorption in sediments, two adsorption isotherm models, i.e., the modified Langmuir model and the Freundlich model were used to fit the adsorption characteristics of P. According to Table 3, both adsorption isotherm models can fit sediment isotherm adsorption pattern well.

The modified Langmuir model can be used to describe both single- and deep-layer adsorption on uneven surfaces because it assumes that (i) the surface of the adsorbent is uniform and the number of adsorption sites is limited, (ii) there is no interaction between the adsorbates, and (iii) the adsorption behavior is surface single-layer adsorption (Li et al. 2019b), whereas the Freundlich model assumes there are possible interactions between adsorbed molecules with

Table 3 Parameters of P adsorption isotherm on sediments

Site	Modified Langmuir model			Freundlich model			NAP	EPC ₀
	S _{max}	k _d	r ²	K _F	1/n	r ²		
A1	415.7533	9.5308	0.9741	41.7092	0.6915	0.9722	16.60	0.40
A2	1226.3769	18.3020	0.9812	78.1741	0.7442	0.9865	19.62	0.30
A3	711.7100	7.8663	0.9904	104.7234	0.5891	0.9966	7.63	0.09
A4	584.6161	6.1606	0.9903	94.4941	0.5766	0.9850	19.36	0.21
A5	848.6725	8.5909	0.9814	106.7155	0.6315	0.9850	20.11	0.21
A6	460.7176	5.0092	0.9818	90.8256	0.5256	0.9846	17.70	0.20
B1	488.4604	4.9017	0.9769	97.7774	0.5218	0.9847	21.63	0.23
B2	1037.1198	5.6115	0.9964	200.1133	0.5285	0.9922	7.29	0.04
B3	732.5846	4.3162	0.9963	173.8686	0.4742	0.9961	14.65	0.09
B4	1172.9591	8.7848	0.9951	140.3064	0.6448	0.9943	32.73	0.25
B5	731.0135	5.8195	0.9979	128.1587	0.5553	0.9949	20.34	0.17

S_{max} the maximum P adsorption capacity at saturation conditions per mass unit of sediment of modified Langmuir model (mg/kg), k_d the empirical constant of modified Langmuir model (mg/L), K_F adsorption partition coefficient of Freundlich model, 1/n adsorption exponent ((mg/kg) (mg/L)^{1/n}), NAP native adsorbed exchangeable P, EPC₀ the zero equilibrium P concentration

surface heterogeneity (Li et al. 2020). According to the r^2 fitted using the modified Langmuir model and Freundlich model (Table 3), there is uniform monolayer adsorption on the surface and irregular multilayer adsorption on the surface in the P adsorption process. From the variations in the fitted r^2 of the two models (Table 3), except for site B1, sediments at other sites in the Lengshui River are fitted well using the modified Langmuir model, indicating the P adsorption process by the sediments in the Lengshui River is dominated by uniform single-layer adsorption on the surface, except for sites A2 and A4. The adsorption processes at other sites in Muiyang River are more fitted better using the Freundlich model, suggesting that the P adsorption process by the sediments in the Muiyang River is dominated by irregular multilayer adsorption on the surface at the same time.

In the modified Langmuir model, S_{\max} represents the maximum P saturation adsorption capacity of sediments (Zhou et al. 2005). The average S_{\max} of Muiyang River sediments is 707.9744 mg kg⁻¹, while average S_{\max} of Lengshui River sediments is 832.4275 mg kg⁻¹, indicating that the Lengshui River sediments can adsorb more P than the Muiyang River.

According to K_F and $\frac{1}{n}$ values of the Freundlich model, the ability of sediments to adsorb P and the ease of the adsorption reaction can be inferred, respectively (Wang et al. 2019a). K_F represents P adsorption capacity of sediments, which is ranked in sequence as follows: B2 > B3 > B4 > B5 > A5 > A3 > B1 > A4 > A6 > A2 > A1. Overall, the Lengshui River sediment is more P-absorbing than Muiyang River sediments. In terms of $\frac{1}{n}$, the P adsorption reaction in the sediments occurs in the following order: B3 > B1 > A6 > B2 > B5 > A4 > A3 > A5 > B4 > A1 > A2. The Lengshui River sediment adsorbs phosphates more easily than Muiyang River sediments.

By fitting the parameters of sediment P adsorption thermodynamics, sediment NAP and EPC₀ can be calculated. Thus, this further reveals whether the sediment is a “source” or “sink” in the water body (Pan et al. 2013). As shown in Table 3, NAP is ranked from high to low: B4 > B1 > B5 > A5 > A2 > A4 > A5 > A1 > B3 > A3 > B2. The average NAP of the six samples sites in the Muiyang River is 16.8306 mg kg⁻¹, whereas the average NAP of the five sampling sites in the Lengshui River is 19.3277 mg kg⁻¹, indicating that the Ex-P concentration in the Lengshui River sediments is higher than that in the Muiyang River. Comparing the EPC₀ with the TP concentration in water (Hao et al. 2014; Du 2020), sediments at 11 sites are all the “sources” of P to the overlying water, that is, these sediments tend to release P into the water body.

Studies have shown that intensive farming and high-intensity precipitation will increase soil erosion, resulting in higher soil clay content, which will increase the content of metal oxides (Didoné et al. 2014). In fact, there are severe

soil erosion in the watershed found in this study. After erosion, soil enters the river channel and settles on the river bed to form sediments (Lamba et al. 2015). Figure 1 and Table 1 show that the density of residential areas and farmland near the Lengshui River is higher than those near the Muiyang River, and the concentrations of CaO, TFe₂O₃, and Al₂O₃ in sediments in the Lengshui River are higher than those in the Muiyang River. The P adsorption capacity of Lengshui River sediments is also stronger than that of Muiyang River sediments. This may be attributed to human activities that increase the content of metal oxides in sediments, allowing the sediments to retain more P. This is consistent with the results from a previous study by Zafar et al. (2016) on sediment P adsorption–desorption kinetics by land use and management in Guapore catchment, Brazil. Although human activities have enhanced the sediment P retention capacity, the main form of P speciation is Fe/Al-P that is the P fraction with high bioavailability in sediments. It was easy to decompose and release phosphate, which posed a high threat to water bodies. The finding from this study is consistent with those from other regions around the world that agricultural activities increase the bioavailability and mobility of P in sediments, enhancing P desorption capacity and pose a major threat to water quality (Lehtoranta et al. 2015; Weigelhofer 2017; Kreiling et al. 2019; Casillas-Ituarte et al. 2020).

3.5 Relationship between sediment properties, phosphorus fractions, and adsorption characteristics

Principle component analysis (PCA) is used in this study to explore the relationship between sediment properties and P fractions. Extracted principal components is used to perform an in-depth analysis of the correlation between variables whose cumulative explanatory variance is greater than 70% and the absolute value of the factor loading is greater than 0.6.

Table 4 shows that factor 1 mainly reflects that sediment TP, Auth-P, Detr-P, and Res-P changes in the same trend. The linear correlation analysis shows that there is a significant positive correlation between sediment TP and Auth-P, Detr-P, and Res-P ($p < 0.05$) (Table 6). Although few studies have been conducted on sediments in the same study area, research conducted on sediments from the Dian Lake basin has suggested that sediment TP mainly exists in the form of Ca-P and Org-P (Yang et al. 2017). Since Auth-P and Detr-P in this study are P complexed with calcium chemicals in the sediments (Loh et al. 2020) and some Res-P in this study is P from organic compounds in the sediments (Meis et al. 2012), the results from this study are consistent with other findings from sediment research in the Dian Lake basin (Gao et al. 2005; Liu et al. 2016; Zhu et al. 2018). Since, Auth-P, Detr-P, and Res-P cannot be mineralized by microorganisms

Table 4 PCA characteristic loading of basic physical and chemical properties and phosphorus fractions of sediments

Parameters	Factor 1	Factor 2	Factor 3
OM	0.287618	0.234364	0.850639
TP	0.809908	0.435103	0.271234
CaO	-0.531226	0.044325	0.763178
TFe ₂ O ₃	0.515615	0.787795	0.125171
Al ₂ O ₃	0.251825	0.736991	-0.113288
Ex-P	0.349775	-0.255130	0.802582
Al-P	0.487664	0.798344	0.237293
Fe-P	0.491687	0.793070	-0.147851
Auth-P	0.839866	0.210404	0.241346
Detr-P	0.817845	0.362074	-0.071855
Org-P	-0.041969	-0.808906	-0.070812
Res-P	0.780078	0.331814	0.093299
Total variation explained	32.8%	30.7%	18.4%

in neutral to alkaline weak pH environment (Kim et al. 2003; Barik et al. 2019; Saha et al. 2021), these P fractions will be rather stable under the sediment environment of this study (Table 1). Factor 2 mainly reflects the variation trends between TFe₂O₃ and Al₂O₃ and shows that Fe-P and Al-P are in the same direction, whereas TFe₂O₃, Al₂O₃, Fe-P, and Al-P exhibit opposite variation trends with Org-P. Linear correlation analysis shows that TFe₂O₃ and Al₂O₃ and Fe-P and Al-P have a significant positive correlation ($p < 0.05$) (Table 6). Since Fe-P and Al-P are referred to P fractions combined with Fe and Al oxides, the more TFe₂O₃ and Al₂O₃ content in sediments, the more Fe-P and Al-P fractions there will be (Smolders et al. 2006; Yang et al. 2018). In contrast, Org-P is significantly negatively correlated with TFe₂O₃, Al₂O₃, Fe-P, and Al-P ($p < 0.05$), possibly because metal ions promote the hydrolysis of organophosphorus by catalyzing nucleophilic substitution reactions (Zhu et al. 2015; Zhao et al. 2019). Factor 3 mainly shows that sediment OM, CaO, and Ex-P exhibit the same change trend. The linear correlation analysis shows that the sediment OM and CaO and Ex-P have a significant positive correlation ($p < 0.05$) (Table 6). Typically, organic matter and calcium carbonate surface in sediments can provide binding sites for P (Pettersson 2001). However, since the binding force of these binding sites is poor, bonded P can be easily released into the surrounding water under even the slightest environmental disturbance (Zhou et al. 2016). This easily released P fraction is Ex-P (Zhang et al. 2012). Therefore, the Ex-P concentration in sediments is significantly positively correlated with OM and CaO.

Another PCA is performed to analyze the relationship between the occurrence of P in sediments and sediments' P adsorption characteristics. Although the correlation relationship is explored, extracted principal components is further

used to conduct an in-depth analysis of the correlation between variables with an absolute value of factor loading greater than 0.6 among factors with a cumulative explanatory variance of more than 70%.

Table 5 shows that factor 1 mainly reflects the changes in sediment Al-P, Fe-P and adsorption features q_{e2} , k_2 , k_3 , and K_F have the same trend. The linear correlation analysis shows that the sediments Al-P and Fe-P have a significant positive correlation with q_{e2} , k_2 , k_3 , and K_F , respectively ($p < 0.05$) (Table 6). The results suggest that Al-P and Fe-P dominate chemical P adsorption in sediments and control the amount, rate, and strength of the adsorption. The mechanism may be explained by the formation of Fe/Al-P, which is a chemical process depending on complex bonds between iron-aluminum oxides and phosphates (Wu et al. 2014), and the adsorption characteristics (q_{e2} and k_2) indicated by the pseudo-second-order kinetic model, which is chemical adsorption. The results indicate that the entire chemical adsorption process is dominated by Fe/Al-P. Fe/Al-P is mainly formed when P is adsorbed by sediments. The more Fe/Al-P generated by sediments through chemical adsorption, the greater the amount of P adsorbed through chemical adsorption. The faster the rate of Fe/Al-P generation, the faster the rate of chemical adsorption. Because of the large bond energy, good stability, and strong adsorption capacity of the Fe/Al-P fraction, this P fraction will affect the binding rate (q_{e2} , k_2 , and k_3) and adsorption capacity (K_F) of P. This result is consistent with that of Cao et al.

Table 5 PCA characteristic loading of phosphorus fractions and adsorption characteristics of sediments

	Factor 1	Factor 2	Factor 3
Ex-P	-0.402515	0.598991	-0.072776
Al-P	0.718340	0.476895	-0.321531
Fe-P	0.883677	0.270343	-0.260842
Auth-P	0.264324	0.861586	0.001802
Detr-P	0.567480	0.566081	-0.258326
Org-P	-0.365697	-0.197767	0.668265
Res-P	0.537318	0.597759	-0.079139
q_1	-0.023064	0.839519	-0.068474
k_1	0.330984	0.627615	-0.273071
q_2	0.645877	0.554476	-0.330047
k_2	0.778778	-0.038300	-0.200563
k_3	0.785244	-0.082848	-0.172837
S_{max}	0.359220	0.496044	0.634261
k_4	-0.170362	-0.352079	0.886178
K_F	0.786305	0.388755	-0.367861
$\frac{1}{n}$	-0.308990	-0.036107	0.911041
NAP	-0.384214	-0.109967	-0.245094
EPC ₀	-0.473574	-0.489738	0.590196
Total variation explained	29.3%	23.9%	19.5%

Table 6 Results of Pearson correlation coefficient between basic characteristics/adsorption characteristics and P fraction of sediments

	Ex-P	Al-P	Fe-P	Auth-P	Detr-P	Org-P	Res-P
OM	0.650**	0.511**		0.561**			
TP	0.404*	0.823**	0.720**	0.799**	0.773**	-0.418**	0.778**
CaO	0.360*				-0.424*		
TFe ₂ O ₃		0.950**	0.907**	0.616**	0.698**	-0.533**	0.663**
Al ₂ O ₃		0.589**	0.634**	0.382*	0.411**	-0.560**	0.409*
q_1		0.417*		0.628**	0.396*		
k_1	0.386*	0.561**	0.503**	0.554**	0.668**	-0.437*	0.533**
q_2		0.845**	0.822**	0.598**	0.664**	-0.562**	0.609**
k_2		0.674**	0.748**		0.531**		0.521**
k_3		0.576**	0.693**			-0.458*	0.372*
S_{\max}				0.525**			0.356*
k_4		-0.542**	-0.468**	-0.361*	-0.538**	0.679**	-0.403*
K_F		0.905**	0.937**	0.554**	0.697**	-0.601**	0.586**
$\frac{1}{n}$		-0.496**	-0.511**		-0.452**	0.643**	

*Significant at the 0.05 level

**Significant at the 0.01 level

(2017). Factor 2 mainly reflects the variation trends in sediment Auth-P although q_{e1} and k_1 are the same. The linear correlation analysis shows that there is a significant positive correlation between the sediment Auth-P and q_{e1} and k_1 ($p < 0.05$) (Table 6). This indicates that Auth-P dominates the physical sediment adsorption process and can affect the adsorption amount and rate. The mechanism may be explained by Auth-P, which was among P fractions, co-precipitates with calcium carbonate. The adsorption process mainly depends on the surface sites on calcium carbonate, which adsorbs phosphate through van der Waals (Tolls 2001), inductive, and dispersion forces (Yang et al. 2016). The adsorption characteristics (q_{e1} and k_1) indicated by the pseudo-first-order kinetic model is physical adsorption (Wu et al. 2016). The more Auth-P generated by sediments through physical adsorption, the greater the amount of P adsorbed through physical adsorption; the faster the rate of Auth-P generation, the faster the rate of physical adsorption. The significant correlation between Auth-P and q_{e1} and k_1 suggests that the physical adsorption of P by sediments is mainly related to calcium carbonate adsorption sites in sediments. Therefore, the amount of P adsorbed (q_{e1}) along with the P binding rate (k_1) will be affected by calcium carbonate (Liu et al. 2012). Factor 3 mainly implies that the trends of variations of Org-P, S_{\max} , k_4 , and $\frac{1}{n}$ were the same. The linear correlation analysis shows that there is a significant positive correlation between the sediment Org-P and S_{\max} , k_4 , and $\frac{1}{n}$ ($p < 0.05$) (Table 6). The result suggests that Org-P can affect the maximum P adsorption capacity, rate, and strength. The possible mechanism is that sediment maximum P adsorption capacity is positively related to Org-P because Org-P may be the main storage form of P in the sediments (Fig. 2). Therefore, there is a relationship between Org-P and the sediment maximum P adsorption capacity. When organic matter binds

to sediment particles, it covers the positively charged surface or binding sites of particles, which results in sediment P and the adsorption process changes from chemisorption to physical adsorption (Ren et al. 2018). On the one hand, the rate of physical adsorption is faster than chemical adsorption. On the other hand, the physical adsorption strength is significantly low (Xu et al. 2019). Therefore, the faster the generation rate of Org-P, the faster the adsorption rate, but the lower the strength of adsorption binding (Zhan et al. 2017).

As indicated by the relationship among P adsorption capacity, P fractions, and sediment properties in the PCA analysis, several strategies can be applied to assist the management of sediment P release risk. Firstly, to increase the sediment P adsorption capacity, organism biomass and diversity, such as submerged plants, benthic animals, and microorganisms in the Lengshui River, can be improved (DiCarlo et al. 2020; Simpson et al. 2020), which can help increase the content of Org-P and the sediment maximum P adsorption capacity. In addition, in order to store more phosphate, appropriate amounts of iron, aluminum, and calcium salts can be added to the sediments in the MUYANG River (Mizuno et al. 1968) to make them more quickly adsorb phosphate that is then further converted into Org-P through the biological process by organisms in the sediments. Secondly, to reduce the P release capacity in the sediments in the two rivers, it is necessary to control soil erosion in the watershed and improve domestic sewage treatment capacity (Fan et al. 2019). This will reduce the concentration of phosphate entering the rivers. In the meantime, it is necessary to take appropriate engineering measures to convert Fe/Al-P to Detr-P (Zhan et al. 2020) in the sediments, which can reduce the bioavailability and mobility of P and then have a positive effect on water quality protection.

4 Conclusions

In this study, sediment P fractionation and adsorption behavior in two major input rivers (the Muyang and Lengshui Rivers) are investigated to provide management suggestions for protection of the Songhua Drinking Water Reservoir. Sediment P fractions and speciation vary in the two rivers. The proportion of Org-P in Muyang River sediment is relatively high, whereas the Lengshui River sediment has higher fractions of Detr-P and Al/Fe-P, indicating that the Lengshui River has experienced intensive human activity interference. Although P adsorption kinetics in the sediments in the Lengshui River and Muyang River is in line with the pseudo-second-order kinetic model, the upper reaches of both rivers are dominated by single-layer adsorption. Increasing interference downstream due to human activities results in the adsorption to gradually become irregular and complex deep adsorption procedure. The results from the modified Langmuir model and Freundlich model indicate that the characteristics of sediment P adsorption isotherm vary between these two rivers. The affinity and maximum P adsorption capacity in the sediments are higher in the Lengshui River than that in Muyang River. The results also show that EPC_0 values in both river sediments are higher than P concentration in the overlying water, suggesting that the sediments tend to release orthophosphate into the overlying water body. PCA shows that sediment P fraction features correlate with several P adsorption characteristics. Firstly, the Fe/Al-P fraction in sediments positively correlates with equilibrium adsorption capacity, rate, and strength. Then, the rate and amount of sediment physical P adsorption increase with the Auth-P fraction in the sediment. Finally, the maximum adsorption capacity of P in sediments is positively influenced by Org-P.

Therefore, engineering measures, such as increasing domestic sewage treatment capacity, growing macrophyte, introducing benthic organisms, and using sediment property modifiers, can convert high bioavailable Fe/Al-P to low bioavailable Detr-P, which may help reduce the risk of P release from sediments and further protect water quality of the drinking the water source reservoir.

Supplementary information The online version contains supplementary material available at <https://doi.org/10.1007/s11368-022-03257-1>.

Funding This study was supported by the Basic Research Foundation of Yunnan Province (202101AT070014), the Yunnan Science and Technology Major Project (grant number 2019BC002), and the Key Program of Basic Research Foundation of Yunnan Province (2019FA043).

Declarations

Conflict of interest The authors declare no competing interests.

References

- Abeyasinghe DH, Shanableh A, Rigden B (1996) Biofilters for water reuse in aquaculture. *Water Sci Technol* 34(11):253–260. <https://doi.org/10.2166/wst.1996.0287>
- Acharya SS, Panigrahi MK, Kurian J, Gupta AK, Tripathy S (2016) Speciation of phosphorus in the continental shelf sediments in the Eastern Arabian Sea. *Cont Shelf Res* 115:65–75. <https://doi.org/10.1016/j.csr.2016.01.005>
- Bao L, Kang H, Hu X, Zhang N, Zhao X, Xu H (2015) The load estimation of nitrogen and phosphorus from non-point sources in the Songhuaba Reservoir watershed. *Environ Sci Surv* 34(03):1–6 (In Chinese with English Abstract)
- Barbosa VV, Severiano JdS, de Oliveira DA, de Lucena Barbosa JE (2020) Influence of submerged macrophytes on phosphorus in a eutrophic reservoir in a semiarid region: influence of submerged macrophytes on phosphorus. *J Limnol* 79(2). <https://doi.org/10.4081/jlimnol.2020.1931>
- Barik SK, Bramha S, Bastia TK, Behera D, Mohanty PK, Rath P (2019) Distribution of geochemical fractions of phosphorus and its ecological risk in sediment cores of a largest brackish water lake. *South Asia Int J Sediment Res* 34(3):251–261. <https://doi.org/10.1016/j.ijsrc.2018.11.004>
- Cai O, Xiong Y, Yang H, Liu J, Wang H (2020) Phosphorus transformation under the influence of aluminum, organic carbon, and dissolved oxygen at the water-sediment interface: a simulative study. *Front Env Sci Eng* 14(3):50. <https://doi.org/10.1007/s11783-020-1227-z>
- Cao X, Liu X, Zhu J, Wang L, Liu S, Yang G (2017) Characterization of phosphorus sorption on the sediments of Yangtze River Estuary and its adjacent areas. *Mar Pollut Bull* 114(1):277–284. <https://doi.org/10.1016/j.marpolbul.2016.09.026>
- Carpenter SR (2005) Eutrophication of aquatic ecosystems: bistability and soil phosphorus. *Proc Natl Acad Sci USA* 102(29):10002–10005. <https://doi.org/10.1073/pnas.0503959102>
- Casillas-Iuarte NN, Sawyer AH, Danner KM, King KW, Covault AJ (2020) Internal phosphorus storage in two headwater agricultural streams in the Lake Erie Basin. *Environ Sci Technol* 54(1):176–183. <https://doi.org/10.1021/acs.est.9b04232>
- Copetti D, Tartari G, Valsecchi L, Salerno F, Viviano G, Mastroianni D, Yin H, Viganò L (2019) Phosphorus content in a deep river sediment core as a tracer of long-term (1962–2011) anthropogenic impacts: a lesson from the Milan metropolitan area. *Sci Total Environ* 646:37–48. <https://doi.org/10.1016/j.scitotenv.2018.07.256>
- Dai Z, Liu G, Chen H, Chen C, Wang J, Ai S, Wei D, Li D, Ma B, Tang C, Brookes PC, Xu J (2020) Long-term nutrient inputs shift soil microbial functional profiles of phosphorus cycling in diverse agroecosystems. *ISME J* 14:757–770. <https://doi.org/10.1038/s41396-019-0567-9>
- Dan SF, Lan W, Yang B, Han L, Xu C, Lu D, Kang Z, Huang H, Ning Z (2020) Bulk sedimentary phosphorus in relation to organic carbon, sediment textural properties and hydrodynamics in the northern Beibu Gulf. *South China Sea Mar Pollut Bull* 155:111176. <https://doi.org/10.1016/j.marpolbul.2020.111176>
- DiCarlo AM, Weisener CG, Drouillard KG (2020) Evidence for microbial community effect on sediment equilibrium phosphorus concentration (EPC_0). *Bull Environ Contam Toxicol* 105:736–741. <https://doi.org/10.1007/s00128-020-03019-0>
- Didoné EJ, Minella JPG, Reichert JM, Merten GH, Dalbianco L, de Barros CAP, Ramon R (2014) Impact of no-tillage agricultural systems on sediment yield in two large catchments in Southern Brazil. *J Soils Sediments* 14:1287–1297. <https://doi.org/10.1007/s11368-013-0844-6>
- Dittrich M, Chesnyuk A, Gudimov A, McCulloch J, Quazi S, Young J, Winter J, Stainsby E, Arhonditsis G (2013) Phosphorus retention

- in a mesotrophic lake under transient loading conditions: insights from a sediment phosphorus binding form study. *Water Res* 47(3):1433–1447. <https://doi.org/10.1016/j.watres.2012.12.006>
- Du Z (2020) Source apportionment of water environmental pollution and optimization in the inflow rivers of Songhuaba Reservoir of Lake Dianchi Basin. Dissertation, Yunnan University. (In Chinese with English Abstract)
- Duan S, Yang Y, Ma X, Wang J, Li J, Luo S (2019) Research on the water quality trend of input rivers of urban drinking water source of a high plateau city - taking Muyanghe of Songhuaba Reservoir for example. *China Rural Water Hydropower* (03):55–57+62 (In Chinese with English Abstract)
- EPD (2012) Soil-Determination of ammonium, nitrite and nitrate by extraction with potassium chloride solution-spectrophotometric methods. Environmental Protection Department, China. HJ 634–2012. (In Chinese)
- Evans DJ, Johns PJ, Lawrence DS (2004) Physico-chemical controls on phosphorus cycling in two lowland streams. Part 2—The sediment phase. *Sci Total Environ* 329(1–3):165–182. <https://doi.org/10.1016/j.scitotenv.2004.02.023>
- Fan Y, Duan S, Zhang Q (2019) Protection measures of Songhuaba Reservoir drinking water source in Kunming. *Reg Gov* 111–113 (In Chinese with English Abstract)
- Feng W, Wu F, He Z, Song F, Zhu Y, Giesy JP, Wang Y, Qin N, Zhang C, Chen H, Sun F (2018) Simulated bioavailability of phosphorus from aquatic macrophytes and phytoplankton by aqueous suspension and incubation with alkaline phosphatase. *Sci Total Environ* 616–617:1431–1439. <https://doi.org/10.1016/j.scitotenv.2017.10.172>
- Froelich PN (1988) Kinetic control of dissolved phosphate in natural rivers and estuaries: a primer on the phosphate buffer mechanism. *Limnol Oceanogr* 33(4):649–668. <https://doi.org/10.4319/lo.1988.33.4part2.0649>
- Gao L, Zhou JM, Yang H, Chen J (2005) Phosphorus fractions in sediment profiles and their potential contributions to eutrophication in Dianchi Lake. *Environ Geol* 48:835–844. <https://doi.org/10.1007/s00254-005-0005-3>
- Gao Y, Liang T, Tian S, Wang L, Holm PE, Bruun Hansen HC (2016) High-resolution imaging of labile phosphorus and its relationship with iron redox state in lake sediments. *Environ Pollut* 219:466–474. <https://doi.org/10.1016/j.envpol.2016.05.053>
- GAQ and SA (2010) Methods for chemical analysis of silicate rocks — part 28: determination of 16 major and minor elements content. General Administration of Quality Supervision, Inspection and Quarantine of the People's Republic of China and Standardization Administration of the People's Republic of China, China. GB/T 14506.28–2010. (In Chinese)
- Gautreau E, Volatier L, Nogaro G, Gouze E, Mermillod-Blondin F (2020) The influence of bioturbation and water column oxygenation on nutrient recycling in reservoir sediments. *Hydrobiologia* 847:1027–1040. <https://doi.org/10.1007/s10750-019-04166-0>
- Habte D, Kebede F, Bedadi B, Wogi L (2020) Phosphorus sorption-desorption properties of Luvisols and Vertisols, sorption kinetics and models comparison. *Commun Soil Sci Plant Anal* 51(4):527–540. <https://doi.org/10.1080/00103624.2020.1717512>
- Hao F, Shi J, Zhang N, Hu X (2014) Research of nitrogen and phosphorus pollution load from non-point source in the Songhuaba Reservoir Basin. *Environ Sci Surv* 33(06):10–14 (In Chinese with English Abstract)
- Ho Y-S (2006) Review of second-order models for adsorption systems. *J Hazard Mater* 136(3):681–689. <https://doi.org/10.1016/j.jhazmat.2005.12.043>
- Ho YS, McKay G (1999) Pseudo-second order model for sorption processes. *Process Biochem* 34(5):451–465. [https://doi.org/10.1016/S0032-9592\(98\)00112-5](https://doi.org/10.1016/S0032-9592(98)00112-5)
- Hong S, Liang C, Zhang H, Li H, Wu X (2012) Algae-ecological assessment of water quality and influence factors of algae growth in Songhuaba water source region of Yunnan. *J Hydroelectric Eng* 31(2):152–158 (In Chinese with English Abstract)
- Hu P, Wang L, Li Z, Zhu H, Tang H (2018) Numerical simulation of the interaction between phosphorus and sediment based on the modified Langmuir equation. *Water* 10(7):840. <https://doi.org/10.3390/w10070840>
- Jin X, Wang S, Pang Y, Chang WuF (2006) Phosphorus fractions and the effect of pH on the phosphorus release of the sediments from different trophic areas in Taihu Lake. *China Environ Pollut* 139(2):288–295. <https://doi.org/10.1016/j.envpol.2005.05.010>
- Jin X, He Y, Kirumba G, Hassan Y, Li J (2013) Phosphorus fractions and phosphate sorption-release characteristics of the sediment in the Yangtze River estuary reservoir. *Ecol Eng* 55:62–66. <https://doi.org/10.1016/j.ecoleng.2013.02.001>
- Kastelan-Macan M, Petrovic M (1996) The role of fulvic acids in phosphorus sorption and release from mineral particles. *Water Sci Technol* 34(7–8):259–265. <https://doi.org/10.2166/wst.1996.0630>
- Kaiserli A, Voutsas D, Samara C (2002) Phosphorus fractionation in lake sediments – Lakes Volvi and Koronia. *N Greece Chemosphere* 46(8):1147–1155. [https://doi.org/10.1016/S0045-6535\(01\)00242-9](https://doi.org/10.1016/S0045-6535(01)00242-9)
- Kang X, Song J, Yuan H, Shi X, Yang W, Li X, Li N, Duan L (2017) Phosphorus speciation and its bioavailability in sediments of the Jiaozhou Bay. *Estuar Coast Shelf Sci* 188:127–136. <https://doi.org/10.1016/j.ecss.2017.02.029>
- Kim LH, Choi E, Stenstrom MK (2003) Sediment characteristics, phosphorus types and phosphorus release rates between river and lake sediments. *Chemosphere* 50(1):53–61. [https://doi.org/10.1016/S0045-6535\(02\)00310-7](https://doi.org/10.1016/S0045-6535(02)00310-7)
- Köse TE, Kıvanç B (2011) Adsorption of phosphate from aqueous solutions using calcined waste eggshell. *Chem Eng J* 178:34–39. <https://doi.org/10.1016/j.cej.2011.09.129>
- Kreiling RM, Thoms MC, Bartsch LA, Richardson WB, Christensen VG (2019) Complex response of sediment phosphorus to land use and management within a river network. *J Geophys Res Biogeosci* 124(7):1764–1780. <https://doi.org/10.1029/2019JG005171>
- Lagergren S (1898) Zur theorie der sogenannten adsorption gelöster stoffe kungliga svenska vetenskapsakademiens. *Handlingar* 24(4):1–39
- Lamba J, Karthikeyan KG, Thompson AM (2015) Apportionment of suspended sediment sources in an agricultural watershed using sediment fingerprinting. *Geoderma* 239–240:25–33. <https://doi.org/10.1016/j.geoderma.2014.09.024>
- Lao J (1988) Handbook of soil agrochemical analysis. China. (In Chinese)
- Le C, Zha Y, Li Y, Sun D, Lu H, Yin B (2010) Eutrophication of lake waters in China: cost, causes, and control. *Environ Manage* 45:662–668. <https://doi.org/10.1007/s00267-010-9440-3>
- Lehtoranta J, Ekholm P, Wahlström S, Tallberg P, Uusitalo R (2015) Labile organic carbon regulates phosphorus release from eroded soil transported into anaerobic coastal systems. *Ambio* 44:263–273. <https://doi.org/10.1007/s13280-014-0620-x>
- Leote C, Epping E, Van Cappellen P (2013) Phosphate sorption from seawater solutions: Particle concentration effect. *Mar Chem* 148:52–62. <https://doi.org/10.1016/j.marchem.2012.12.002>
- Li A, Li S, Yu B, Ma A, Zhou X, Xie J, Jiang Y, Deng H (2020) Adsorption of ammonia nitrogen and phosphorus by magnesium impregnated biochar: preparation optimization and adsorption mechanism. *Ciesc J* 71(04):1683–1695 (In Chinese with English Abstract)
- Li H, Yang G, Ma J, Wei Y, Kang L, He Y, He Q (2019a) The role of turbulence in internal phosphorus release: turbulence intensity matters. *Environ Pollut* 252:84–93. <https://doi.org/10.1016/j.envpol.2019.05.068>

- Li J, Werth CJ (2002) Modeling sorption isotherms of volatile organic chemical mixtures in model and natural solids. *Environ Toxicol Chem* 21(7):1377–1383. <https://doi.org/10.1002/etc.5620210707>
- Li S, Fang B, Wang D, Wang X, Man X, Zhang X (2019b) Leaching characteristics of heavy metals and plant nutrients in the sewage sludge immobilized by composite phosphorus-bearing materials. *Int J Environ Res Public Health* 16(24):5159. <https://doi.org/10.3390/ijerph16245159>
- Li X, Guo M, Duan X, Zhao J, Hua Y, Zhou Y, Liu G, Dionysiou DD (2019c) Distribution of organic phosphorus species in sediment profiles of shallow lakes and its effect on photo-release of phosphate during sediment resuspension. *Environ Int* 130:104916. <https://doi.org/10.1016/j.envint.2019.104916>
- Li X, Huang L, Fang H, Chen M, Cui Z, Sun Z, Reible D (2021) Phosphorus adsorption by sediment considering mineral composition and environmental factors. *Environ Sci Pollut Res* 28:17495–17505. <https://doi.org/10.1007/s11356-020-12206-9>
- Li Y, Wu D, Xue Y (1998) A development sequential extraction method for different forms of phosphorus in the sediments and its environmental geochemical significance. *Mar Environ Sci* 01:16–21 (In Chinese with English Abstract)
- Liu J, Luo X, Zhang N, Wu Y (2016) Phosphorus released from sediment of Dianchi Lake and its effect on growth of *Microcystis aeruginosa*. *Environ Sci Pollut Res* 23:16321–16328. <https://doi.org/10.1007/s11356-016-6816-9>
- Liu Q, Guo L, Zhou Y, Dai Y, Feng L, Zhou J, Zhao J, Liu J, Qian G (2012) Phosphate adsorption on biogenetic calcium carbonate minerals: effect of a crystalline phase. *Desalin Water Treat* 47(1–3):78–85. <https://doi.org/10.1080/19443994.2012.696798>
- Liu R, Hao X, Chen Q, Li J (2019a) Research advances of *Tetrasphaera* in enhanced biological phosphorus removal: a review. *Water Res* 166:115003. <https://doi.org/10.1016/j.watres.2019.115003>
- Liu X, Shen F, Smith RL Jr, Qi X (2019b) Black liquor-derived calcium-activated biochar for recovery of phosphate from aqueous solutions. *Bioresour Technol* 294:122198. <https://doi.org/10.1016/j.biortech.2019.122198>
- Logan TJ (1982) Mechanisms for release of sediment-bound phosphate to water and the effects of agricultural land management on fluvial transport of particulate and dissolved phosphate. *Hydrobiologia* 91:519–530. <https://doi.org/10.1007/PL00020041>
- Loh PS, Huang X-R, Ying C-Y, Hu J, Lou Z-H, Chen X-G, He S, Jiang Z-P, Jin A-M (2020) Sources, distribution and bioavailability of sedimentary phosphorus species in coastal areas off Changjiang Estuary. *SN Appl Sci* 2:1280. <https://doi.org/10.1007/s42452-020-3090-8>
- Long Y, Hu X, Jiang J, Hu J, Zhu C, Zhou S (2021) Phosphorus sorption - desorption behaviors in the sediments cultured with *Hydrilla verticillata* and *Scripus triquetus* as revealed by phosphorus fraction and dissolved organic matter. *Chemosphere* 271:129549. <https://doi.org/10.1016/j.chemosphere.2021.129549>
- Meis S, Spears BM, Maberly SC, O'Malley MB, Perkins RG (2012) Sediment amendment with Phoslock® in Clatto Reservoir (Dundee, UK): investigating changes in sediment elemental composition and phosphorus fractionation. *J Environ Manage* 93(1):185–193. <https://doi.org/10.1016/j.jenvman.2011.09.015>
- Meng R, Dennison PE, Huang CQ, Moritz MA, D'Antonio C (2015) Effects of fire severity and post-fire climate on short-term vegetation recovery of mixed-conifer and red fir forests in the Sierra Nevada Mountains of California. *Remote Sens Environ* 171:311–325. <https://doi.org/10.1016/j.rse.2015.10.024>
- Mizuno S, Yamazaki H, Nitta K, Umezawa H (1968) Inhibition of initiation of DNA-dependent RNA synthesis by an antibiotic B44P. *Biochem Biophys Res Commun* 30(4):379–385. [https://doi.org/10.1016/0006-291X\(68\)90755-9](https://doi.org/10.1016/0006-291X(68)90755-9)
- NFB (1999) Determination of organic matter in forest soil and calculation carbon-nitrogen ratio. Nation forestry Bureau 1999. LY/T 1237–1999. (In Chinese)
- Ni Z, Wang S, Zhang M (2016) Sediment amino acids as indicators of anthropogenic activities and potential environmental risk in Erhai Lake, Southwest China. *Sci Total Environ* 551–552:217–227. <https://doi.org/10.1016/j.scitotenv.2016.02.005>
- Ni Z, Wang S, Wu Y, Pu J (2020) Response of phosphorus fractionation in lake sediments to anthropogenic activities in China. *Sci Total Environ* 699:134242. <https://doi.org/10.1016/j.scitotenv.2019.134242>
- Padmash TVN, Vijayaraghavan K, Sekaran G, Velan M (2005) Batch and column studies on biosorption of acid dyes on fresh water macro alga *Azolla filiculoides*. *J Hazard Mater* 125(1–3):121–129. <https://doi.org/10.1016/j.jhazmat.2005.05.014>
- Pan G, Krom MD, Zhang M, Zhang X, Wang L, Dai L, Sheng Y, Mortimer RJ (2013) Impact of suspended inorganic particles on phosphorus cycling in the Yellow River (China). *Environ Sci Technol* 47(17):9685–9692. <https://doi.org/10.1021/es4005619>
- Pereira FG, Amarakoon ID, Zvomuya F, Jeke NN (2018) Kinetics and thermodynamics of phosphorus sorption on goethites: effects of biochar application. *Can J Soil Sci* 98(1):128–135. <https://doi.org/10.1139/cjss-2017-0094>
- Pettersson K (2001) Phosphorus characteristics of settling and suspended particles in Lake Erken. *Sci Total Environ* 266(1–3):79–86. [https://doi.org/10.1016/S0048-9697\(00\)00737-3](https://doi.org/10.1016/S0048-9697(00)00737-3)
- Petticrew EL, Arocena JM (2001) Evaluation of iron-phosphate as a source of internal lake phosphorus loadings. *Sci Total Environ* 266(1–3):87–93. [https://doi.org/10.1016/S0048-9697\(00\)00756-7](https://doi.org/10.1016/S0048-9697(00)00756-7)
- Pu J, Ni Z, Wang S (2020) Characteristics of bioavailable phosphorus in sediment and potential environmental risks in Poyang Lake: the largest freshwater lake in China. *Ecol Indic* 115:106409. <https://doi.org/10.1016/j.ecolind.2020.106409>
- Qiu X, Fu B, Xia T, He S, Yu X, Lu Y (2012) Spatial-temporal variations of water quality in Muyang River of Songhuaba Reservoir. *J Soil Water Conserv* 26(1):255–258 (In Chinese with English Abstract)
- Reddy KR, Kadlec RH, Flaig E, Gale PM (1999) Phosphorus retention in streams and wetlands: a review. *Crit Rev Environ Sci Technol* 29(1):83–146. <https://doi.org/10.1080/10643389991259182>
- Ren X, Zeng G, Tang L, Wang J, Wan J, Liu Y, Yu J, Yi H, Ye S, Deng R (2018) Sorption, transport and biodegradation - an insight into bioavailability of persistent organic pollutants in soil. *Sci Total Environ* 610–611:1154–1163. <https://doi.org/10.1016/j.scitotenv.2017.08.089>
- Ren Z, Fu W (2017) Trend analysis of water quality and water pollution control of Songhuaba Reservoir. *Environ Sci Surv* 36(01):18–20 (In Chinese with English Abstract)
- Ruban V, López-Sánchez JF, Pardo P, Rauret G, Muntau H, Quevauviller P (2001) Harmonized protocol and certified reference material for the determination of extractable contents of phosphorus in freshwater sediments – a synthesis of recent works. *Fresenius J Anal Chem* 370:224–228. <https://doi.org/10.1007/s002160100753>
- Ruttenberg KC (1992) Development of a sequential extraction method for different forms of phosphorus in marine sediments. *Limnol Oceanogr* 37(7):1460–1482. <https://doi.org/10.4319/lo.1992.37.7.1460>
- Rydin E (2000) Potentially mobile phosphorus in Lake Erken sediment. *Water Res* 34(7):2037–2042. [https://doi.org/10.1016/S0043-1354\(99\)00375-9](https://doi.org/10.1016/S0043-1354(99)00375-9)
- Saha A, Jesna PK, Ramya VL, Mol SS, Panikkar P, Vijaykumar ME, Sarkar UK, Das BK (2021) Phosphorus fractions in the sediment of a tropical reservoir, India: implications for pollution source identification and eutrophication. *Environ Geochem Health* 44:749–769. <https://doi.org/10.1007/s10653-021-00985-0>

- Selig U (2003) Particle size-related phosphate binding and P-release at the sediment–water interface in a shallow German lake. *Hydrobiologia* 492:107–118. <https://doi.org/10.1023/A:1024865828601>
- Sharpley A, Jarvie HP, Buda A, May L, Spears B, Kleinman P (2013) Phosphorus legacy: overcoming the effects of past management practices to mitigate future water quality impairment. *J Environ Qual* 42(5):1308–1326. <https://doi.org/10.2134/jeq2013.03.0098>
- Shinohara R, Imai A, Kawasaki N, Komatsu K, Kohzu A, Miura S, Sano T, Satou T, Tomioka N (2012) Biogenic phosphorus compounds in sediment and suspended particles in a shallow eutrophic lake: a ^{31}P -nuclear magnetic resonance (^{31}P NMR) Study. *Environ Sci Technol* 46(19):10572–10578. <https://doi.org/10.1021/es301887z>
- Simpson ZP, McDowell RW, Condrón LM (2020) The biotic contribution to the benthic stream sediment phosphorus buffer. *Biogeochemistry* 151:63–79. <https://doi.org/10.1007/s10533-020-00709-z>
- Simpson ZP, McDowell RW, Condrón LM, McDaniel MD, Jarvie HP, Abell JM (2021) Sediment phosphorus buffering in streams at baseflow: a meta-analysis. *J Environ Qual* 50(2):287–311. <https://doi.org/10.1002/jeq2.20202>
- Smolders AJP, Lamers LPM, Lucassen ECHET, Van Der Velde G, Roelofs JGM (2006) Internal eutrophication: how it works and what to do about it—a review. *Chem Ecol* 22(2):93–111. <https://doi.org/10.1080/02757540600579730>
- Song K, Adams CJ, Burgin AJ (2017) Relative importance of external and internal phosphorus loadings on affecting lake water quality in agricultural landscapes. *Ecol Eng* 108:482–488. <https://doi.org/10.1016/j.ecoleng.2017.06.008>
- Søndergaard M, Bjerring R, Jeppesen E (2013) Persistent internal phosphorus loading during summer in shallow eutrophic lakes. *Hydrobiologia* 710:95–107. <https://doi.org/10.1007/s10750-012-1091-3>
- Su J, van Bochove E, Auclair J-C, Thériault G, Denault J-T, Bossé C, Li X, Hu C (2014) Phosphorus algal availability and release potential in suspended and streambed sediments in relation to sediment and catchment characteristics. *Agric Ecosyst Environ* 188:169–179. <https://doi.org/10.1016/j.agee.2014.03.001>
- Tang X, Wu M, Dai X, Chai P (2014) Phosphorus storage dynamics and adsorption characteristics for sediment from a drinking water source reservoir and its relation with sediment compositions. *Ecol Eng* 64:276–284. <https://doi.org/10.1016/j.ecoleng.2014.01.005>
- Taylor AW, Kunishi HM (1971) Phosphate equilibria on stream sediment and soil in a watershed draining an agricultural region. *J Agric Food Chem* 19(5):827–831. <https://doi.org/10.1021/jf60177a061>
- Tolls J (2001) Sorption of veterinary pharmaceuticals in soils: a review. *Environ Sci Technol* 35(17):3397–3406. <https://doi.org/10.1021/es0003021>
- Turner RE, Rabalais NN, Justic D, Dortch Q (2003) Global patterns of dissolved N, P and Si in large rivers. *Biogeochemistry* 64:297–317. <https://doi.org/10.1023/A:1024960007569>
- USEPA (1993) Determination of nitrate-nitrite nitrogen by automated colorimetry. Environmental Protection Agency, U.S
- Vink S, Chambers RM, Smith SV (1997) Distribution of phosphorus in sediments from Tomales Bay. *California Mar Geol* 139(1–4):157–179. [https://doi.org/10.1016/S0025-3227\(96\)00109-0](https://doi.org/10.1016/S0025-3227(96)00109-0)
- Wang G, Gao J, Yang R, Zhang J, Guo H, Gao J (2019a) Preparation of sustainable non-combustion filler substrate from waterworks sludge/aluminum slag/gypsum/silica/maifan stone for phosphorus immobilization in constructed wetlands. *Water Sci Technol* 80(1):153–163. <https://doi.org/10.2166/wst.2019.258>
- Wang H, Dai L, Zhang Y (2019b) Analysis of the cause of exceeded TN concentration and countermeasures in Songhuaba Reservoir. *Environ Sci Surv* 38(S2):42–47 (In Chinese with English Abstract)
- Wang Q, Li Y (2010) Phosphorus adsorption and desorption behavior on sediments of different origins. *J Soils Sediments* 10:1159–1173. <https://doi.org/10.1007/s11368-010-0211-9>
- Wang S, Jin X, Zhao H, Wu F (2006) Phosphorus fractions and its release in the sediments from the shallow lakes in the middle and lower reaches of Yangtze River area in China. *Colloid Surf A-Physicochem Eng Asp* 273(1–3):109–116. <https://doi.org/10.1016/j.colsurfa.2005.08.015>
- Wang X, Zhang L, Zhang H, Wu X, Mei D (2012) Phosphorus adsorption characteristics at the sediment–water interface and relationship with sediment properties in FUSHI reservoir, China. *Environ Earth Sci* 67:15–22. <https://doi.org/10.1007/s12665-011-1476-z>
- Wang X, Wei J, Bai N, Cha H, Cao C, Zheng K, Liu Y (2018) The phosphorus fractions and adsorption-desorption characteristics in the Wuliangshuai Lake, China. *Environ Sci Pollut Res* 25:20648–20661. <https://doi.org/10.1007/s11356-018-2233-6>
- Weigelhofer G (2017) The potential of agricultural headwater streams to retain soluble reactive phosphorus. *Hydrobiologia* 793:149–160. <https://doi.org/10.1007/s10750-016-2789-4>
- Wu H, Xie H, He G, Guan Y, Zhang Y (2016) Effects of the pH and anions on the adsorption of tetracycline on iron-montmorillonite. *Appl Clay Sci* 119:161–169. <https://doi.org/10.1016/j.clay.2015.08.001>
- Wu Y, Priezel J, Zhou J, Bing H, Luo J, Yu D, Sun S, Liang J, Sun H (2014) Soil phosphorus bioavailability assessed by XANES and Hedley sequential fractionation technique in a glacier foreland chronosequence in Gongga Mountain, Southwestern China. *Sci China-Earth Sci* 57:1860–1868. <https://doi.org/10.1007/s11430-013-4741-z>
- Xie F, Dai Z, Zhu Y, Li G, Li H, He Z, Geng S, Wu F (2019) Adsorption of phosphate by sediments in a eutrophic lake: Isotherms, kinetics, thermodynamics and the influence of dissolved organic matter. *Colloid Surf A-Physicochem Eng Asp* 562:16–25. <https://doi.org/10.1016/j.colsurfa.2018.11.009>
- Xiong J, Lin C, Wu Z, Song K, Ma R (2021) Response of phosphorus in estuaries to soil erosion – a new insight into sediment phosphorus fractions and sources. *CATENA* 207:105665. <https://doi.org/10.1016/j.catena.2021.105665>
- Xu R, Zhang Y, Liu R, Cao Y, Wang G, Ji L, Xu Y (2019) Effects of different substrates on nitrogen and phosphorus removal in horizontal subsurface flow constructed wetlands. *Environ Sci Pollut Res* 26:16229–16238. <https://doi.org/10.1007/s11356-019-04945-1>
- Yan K, Yuan Z, Goldberg S, Gao W, Ostermann A, Xu J, Zhang F, Elser J (2019) Phosphorus mitigation remains critical in water protection: a review and meta-analysis from one of China's most eutrophicated lakes. *Sci Total Environ* 689:1336–1347. <https://doi.org/10.1016/j.scitotenv.2019.06.302>
- Yang B, Liu S-M, Wu Y, Zhang J (2016) Phosphorus speciation and availability in sediments off the eastern coast of Hainan Island, South China Sea. *Cont Shelf Res* 118:111–127. <https://doi.org/10.1016/j.csr.2016.03.003>
- Yang C, Yang P, Geng J, Yin H, Chen K (2020) Sediment internal nutrient loading in the most polluted area of a shallow eutrophic lake (Lake Chaohu, China) and its contribution to lake eutrophication. *Environ Pollut* 262:114292. <https://doi.org/10.1016/j.envpol.2020.114292>
- Yang W-Q, Xiao H, Li Y, Miao D-R (2018) Vertical distribution and release characteristics of phosphorus forms in the sediments from the river inflow area of Dianchi Lake. *China Chem Speciation Bioavail* 30(1):14–22. <https://doi.org/10.1080/09542299.2018.1446766>
- Yang Y, Gao B, Hao H, Zhou H, Lu J (2017) Nitrogen and phosphorus in sediments in China: a national-scale assessment and review. *Sci*

- Total Environ 576:840–849. <https://doi.org/10.1016/j.scitotenv.2016.10.136>
- Yuan R (2019) Location-weighted landscape index of non-point source pollution in Songhuaba Reservoir watershed. *Resour Sci* 41(02):405–413 (In Chinese with English Abstract)
- Zafar M, Tiecher T, de Castro Lima JAM, Schaefer GL, Santanna MA, dos Santos DR (2016) Phosphorus seasonal sorption-desorption kinetics in suspended sediment in response to land use and management in the Guaporé catchment. *Southern Brazil Environ Monit Assess* 188:643. <https://doi.org/10.1007/s10661-016-5650-3>
- Zhan Y, Zhang H, Lin J, Zhang Z, Gao J (2017) Role of zeolite's exchangeable cations in phosphate adsorption onto zirconium-modified zeolite. *J Mol Liq* 243:624–637. <https://doi.org/10.1016/j.molliq.2017.08.091>
- Zhan Y, Yu Y, Lin J (2020) Impact of application mode on the control of phosphorus release from sediments using zirconium-modified bentonite as geo-engineering material. *Sci Total Environ* 712:135633. <https://doi.org/10.1016/j.scitotenv.2019.135633>
- Zhang B, Fang F, Guo JS, Chen YP, Li Z, Guo SS (2012) Phosphorus fractions and phosphate sorption-release characteristics relevant to the soil composition of water-level-fluctuating zone of Three Gorges Reservoir. *Ecol Eng* 40:153–159. <https://doi.org/10.1016/j.ecoleng.2011.12.024>
- Zhao G, Sheng Y, Jiang M, Yin X (2019) Redox-dependent phosphorus burial and regeneration in an offshore sulfidic sediment core in North Yellow Sea. *China Mar Pollut Bull* 149:110582. <https://doi.org/10.1016/j.marpolbul.2019.110582>
- Zhou A, Tang H, Wang D (2005) Phosphorus adsorption on natural sediments: modeling and effects of pH and sediment composition. *Water Res* 39:1245–1254. <https://doi.org/10.1016/j.watres.2005.01.026>
- Zhou F, Gao X, Yuan H, Song J, Chen C-TA, Lui H-K, Zhang Y (2016) Geochemical forms and seasonal variations of phosphorus in surface sediments of the East China Sea shelf. *J Mar Syst* 159:41–54. <https://doi.org/10.1016/j.jmarsys.2016.03.005>
- Zhou J, Fan L, Li J (2015) Implementation plan for the construction of drinking water source safety assurance standards for Songhuaba Reservoir in Panlong District, Kunming, Yunnan. *Agric Technol* (17):59–60+65 (In Chinese with English Abstract)
- Zhu G, Yang Y (2018) Variation laws and release characteristics of phosphorus on surface sediment of Dongting Lake. *Environ Sci Pollut Res* 25:12342–12351. <https://doi.org/10.1007/s11356-018-1777-9>
- Zhu M, Zhu G, Li W, Zhang Y, Zhao L, Gu Z (2013) Estimation of the algal-available phosphorus pool in sediments of a large, shallow eutrophic lake (Taihu, China) using profiled SMT fractional analysis. *Environ Pollut* 173:216–223. <https://doi.org/10.1016/j.envpol.2012.10.016>
- Zhu Y, Wu F, He Z, Giesy JP, Feng W, Mu Y, Feng C, Zhao X, Liao H, Tang Z (2015) Influence of natural organic matter on the bioavailability and preservation of organic phosphorus in lake sediments. *Chem Geol* 397:51–60. <https://doi.org/10.1016/j.chemgeo.2015.01.006>
- Zhu Y, Feng W, Liu S, He Z, Zhao X, Liu Y, Guo J, Giesy JP, Wu F (2018) Bioavailability and preservation of organic phosphorus in lake sediments: Insights from enzymatic hydrolysis and ³¹P nuclear magnetic resonance. *Chemosphere* 211:50–61. <https://doi.org/10.1016/j.chemosphere.2018.07.134>

Publisher's Note Springer Nature remains neutral with regard to jurisdictional claims in published maps and institutional affiliations.

Authors and Affiliations

Zihao Fu¹ · Zijin Hong¹ · Junling Wei¹ · Yukai Liao¹ · Songlin You¹ · Yifan Wang¹ · Jianjing Lv¹ · Huan Feng² · Marek Kolenčík³ · Xuexiu Chang^{4,5} · Yu Qian^{1,6}

¹ School of Ecology and Environmental Sciences, Yunnan University, Kunming 650091, Yunnan, China

² Department of Earth and Environmental Studies, Montclair State University, Montclair, NJ 07043, USA

³ Department of Soil Science and Geology, Institute of Agronomic Sciences, Faculty of Agrobiological and Food Resources, Slovak University of Agriculture, Nitra 94976, Slovak Republic

⁴ College of Agronomy and Life Sciences, Kunming University, Kunming 650214, China

⁵ Great Lakes Institute for Environmental Research, University of Windsor, Windsor, ON N9B 3P4, Canada

⁶ Yunnan Key Laboratory for Plateau Mountain Ecology and Restoration of Degraded Environments, Yunnan University, Kunming, Yunnan 650091, China